ARTICLE

Antimicrobial Photodynamic Activity of Gallium-Substituted Haemoglobin on Silver Nanoparticles

Received 00th January 20xx,
Accepted 00th January 20xx

DOI: 10.1039/x0xx00000x

Ana V. Morales-de-Echegaray,[a] Lu Lin,[a] Badhu Sivasubramaniam,[a] Aiga Yermembetova,[a] Qi Wang,[a] Nader S. Abutaleb,[b,c] Mohamed N. Seleem,[b,c] Alexander Wei*[a]

Methicillin-resistant *Staphylococcus aureus* (MRSA), a major scourge in skin and soft-tissue infections, express surface-bound haemoprotein receptors that can be exploited for the targeted delivery of photosensitizers. We have developed a nanosized agent for targeted antimicrobial photodynamic therapy (aPDT), comprised of GaPpIX (a hemin analog with potent photosensitizer activity) encapsulated in haemoglobin (GaHb), mounted on 10-nm Ag nanoparticles (AgNPs). The average GaHb–AgNP contains 28 GaPpIX units stabilized by Hb αβ-dimer units. Eradication (>6-log reduction) of *S. aureus* and MRSA can be achieved by a 10-second exposure to 405-nm irradiation from a light-emitting diode (LED) array (140 mW/cm^2), with GaHb–AgNP loadings as low as 5.6 μg/mL for *S. aureus* and 16.6 μg/mL for MRSA, corresponding to nanomolar levels of GaPpIX. This reduction in bacterial count is several orders of magnitude greater than that of GaHb or free GaPpIX on a per mole basis. The GaHb-AgNP platform is also effective against persister MRSA and intracellular MRSA, and can provide comparable levels of aPDT with a 15-minute irradiation by an inexpensive compact fluorescent lightbulb. Collateral phototoxicity to keratinocytes (HaCaT cells) is low at the GaHb–AgNP concentrations and fluences used for aPDT. GaHb adsorbed on 10-nm AgNPs are much more potent than those on 40-nm AgNPs or 10-nm AuNPs, indicating that both size and plasmon-resonant coupling are important factors for enhanced aPDT. Electron microscopy analysis reveals that GaHb–AgNPs are not readily internalized by *S. aureus* but remain attached to the bacterial cell wall, the likely target of photo-oxidative damage.

Introduction

Staphylococcus aureus and drug-resistant strains such as MRSA continue to be primary threats in healthcare-related infections, despite protracted efforts to reduce the spread of disease.[1] *S. aureus* infections are especially serious in cases of pneumonia and post-surgical infections; a recent study indicates that nearly half of these are MRSA-related.[2] Staphylococcal infections are commonly transmitted by contact, and intervention is possible using topical antibiotics or antiseptics. However, multidrug-resistant *S. aureus* has become decreasingly responsive to these treatments. For example, a growing number of MRSA strains have acquired resistance against mupirocin and chlorhexidine, topical agents used to decolonize superficial bacteria prior to surgery.[3,4]

Antimicrobial photodynamic therapy (aPDT) is a promising alternative for the treatment of exposed or infected tissues.[5,6] aPDT involves the delivery of a photosensitizer (PS) to target bacteria, followed by light irradiation for the localized generation of singlet oxygen ($^1O_2$) or other reactive oxygen species (ROS). All lead to rapid and irreversible oxidative damage: $^1O_2$ is highly energetic and reacts with cell walls and membranes within its proximity, whereas ROS are longer-lived and can degrade metalloproteins and DNA.[7] It is worth noting that there are no specific defence mechanisms against $^1O_2$ because of its short lifetime (microseconds),[8] but sublethal doses can trigger production of repair or antioxidant enzymes that increase bacterial tolerance against oxidative damage.[9,10,11]

aPDT requires photodynamic agents that are potent at low concentrations and have minimal collateral toxicity to host cells, using photon energies and fluences below the threshold for tissue damage. Furthermore, oxidative damage by aPDT is nonspecific but localized, so targeting mechanisms are highly relevant. With respect to $^1O_2$-mediated aPDT, the most appealing target is the cell membrane beneath the bacterial wall or envelope, as damage to this semi-permeable barrier leads to ionic imbalance and disruption in homeostasis.[12] In this regard, aPDT may be most effective by delivering PS systems to specific receptors presented on the bacterial surface.

S. aureus and several other bacterial pathogens are known to express extracellular hemin receptors,[13] which present a mechanism for targeted aPDT. We recently established that GaPpIX, a photoactive analog of hemin, can be taken up by *S. aureus* at diffusion-limited rates.[14] GaPpIX is a highly potent PS against *S. aureus* and MRSA; a 10-second exposure to a 405-

[a] *Department of Chemistry, Purdue University, 560 Oval Drive, West Lafayette, Indiana, 47907-2084, USA.*
[b] *Department of Comparative Pathobiology, Purdue University, 625 Harrison Street, West Lafayette, IN 47907, USA.*
[c] *Department of Biomedical Sciences and Pathobiology, Virginia-Maryland College of Veterinary Medicine, Blacksburg, VA 24061, USA.*

† Footnotes relating to the title and/or authors should appear here.
Electronic Supplementary Information (ESI) available: Synthesis and characterization of GaHb and GaHb–NPs; details on cytotoxicity studies and light sources for aPDT. See DOI: 10.1039/x0xx00000x

nm LED source (140 mW/cm^2) is sufficient to produce a 3-log reduction in bacteria count, with a minimum bactericidal concentration (MBC) below 60 nM.

For further increases in aPDT potency, we considered conjugating GaPpIX to silver nanoparticles (AgNPs), whose plasmon resonance overlaps with the Soret band at 405 nm. Several studies have shown that AgNPs and also gold nanoparticles (AuNPs) are capable of enhancing $^1O_2$ production from nearby PS, separated a few nanometers from the NP surface.[15,16,17,18,19,20] PS–NP complexes can be stabilized by encapsulating PS in porous silica shells[16-18] or by using polyelectrolytes,[21,22] but the encapsulation of GaPpIX compromises its role as a targeting ligand, and the loss of specificity increases NP cytotoxicity.[23] However, direct conjugation of GaPpIX onto metal NPs causes rapid aggregation, so a stabilizing agent is still necessary.

In this paper we use haemoglobin (Hb), a native carrier of haeme, as a stable interface between GaPpIX and 10-nm AgNPs, and evaluate this complex for aPDT against *S. aureus* and several clinical isolates of MRSA (**Figure 1**). Haemoproteins such as Hb are ideal for conjugating GaPpIX onto NP surfaces, for multiple reasons. First, the four subunits of Hb each support a high-affinity binding pocket for haeme or its analogs.[24] Second, NPs *in vivo* are naturally coated by a protein layer or corona, as a consequence of the Vroman effect.[25] Third, several members of the iron-surface determinant (Isd) protein family (the presumed cell-surface hemin receptors on *S. aureus*) have high affinity for haemoproteins such as Hb,[26] ensuring a direct targeting mechanism. The latter feature supports the delivery of the GaPpIX-substituted haemoglobin (GaHb)–AgNP platform to *S. aureus* and MRSA with high affinity.

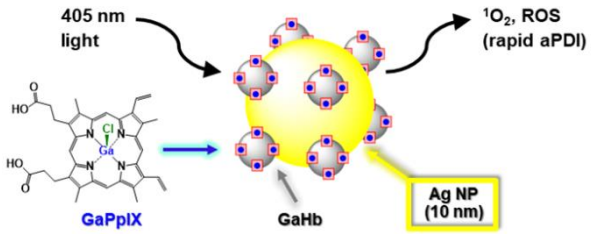

Figure 1. GaPpIX-substituted haemoglobin (GaHb) on Ag nanoparticles for targeted antimicrobial photodynamic therapy (aPDT).

Experimental

All reagents obtained from commercial sources were used as received unless otherwise noted. GaPpIX was prepared according to our previous procedure.[14] *S. aureus* strains were obtained from the American Type Culture Collection (ATCC) or the Biodefense and Emerging Infections (BEI) Research Resources Repository, and cultured at 37 °C in an aerobic atmosphere using tryptic soy broth, supplemented with 3 mM 2,2'-bipyridine to create iron-deficient conditions.

***Instrumentation*.** Optical absorption spectra were collected on a Varian Cary50 spectrometer. Circular dichroism (CD) spectra were obtained using a Jasco J-810 spectrophotometer and collected in triplicate at 25 °C, with data averaging performed after background subtraction; protein samples were prepared in halide-free buffer and diluted to 1 μM. Electron spin resonance (ESR) spectra were obtained using a Bruker EMX X-band spectrometer operating at 9.5 GHz and 5.02 mW, with a modulation amplitude of 5 *g* at 100 kHz. Dynamic light scattering (DLS) and zeta potential measurements were obtained using a Zetasizer Nano ZS system (Malvern) with a 633-nm laser. DLS data was collected at 25 °C, with d_h values based on number-weighted size distributions. Fluorescence polarization (FP) analysis was performed at 25 °C using a Spark 10M multimode microplate reader (Tecan; $\lambda_{ex/em}$ 405/585 nm). Transmission electron microscopy (TEM) images were acquired using a Tecnai T20 (FEI) operating at 200 kV with a charge-coupled device camera (Gatan US1000). Negative TEM staining was performed using 1% phosphotungstic acid. Scanning electron microscopy (SEM) images were acquired using a Helios G4 UX (Thermo Scientific) equipped with an energy dispersive x-ray spectrometer (EDS) operating at 5 V and 0.2 nA. Bacterial specimens were fixed with 5% glutaraldehyde for 30 min, dehydrated by successive rounds of aqueous ethanol washes, then mounted on a plasma-treated Si wafer for SEM analysis.[27]

Preparation of GaHb and GaHb–AgNPs. GaHb was prepared by removing the hemin cofactors from bovine haemoglobin to produce the apoprotein (apoHb) and substituting with GaPpIX, using literature methods.[28,29] Stoichiometric replacement was established by titration and Job plot analysis (see ESI). GaHb–AgNPs were prepared by combining GaHb (1 mg/mL) in phosphate buffered saline (PBS, pH 7.4) with 10- or 40-nm citrate-stabilized AgNPs (20 μg/mL) at 4 °C for 12 h, followed by centrifugation and redispersion in 15 mM borate buffer (pH 8.5). Detailed procedures for the preparation of GaHb and GaHb–AgNPs are described in the ESI.

Antimicrobial photodynamic inactivation assays. All studies were performed in triplicate using 96-well microtiter plates with irradiation from a 405-nm LED array (Rainbow Technology Systems, 140 mW/cm^2) or a 20-W compact fluorescent lightbulb (CFL; Sunlite SL20/BLB) housed in an ellipsoidal reflector dome with emission at 406 nm (*ca.* 12.4 mW/cm^2; see ESI). Assays were performed on planktonic *S. aureus* and MRSA at 10^7 CFU/mL with 10-s irradiation by the LED source or 15-min irradiation by the CFL, followed by plating of serial dilutions and incubation at 37 °C to determine reductions in colony-forming units (CFU). Controls included bacteria without GaHb–AgNPs (Ctrl$^-$), bacteria treated with 0.005% Triton X-100 (TX-100; Ctrl$^+$), and bacteria without light exposure (dark toxicity).

Persister bacteria were generated from the MRSA USA300 strain (NRS 384) by treatment with ciproflaxicin at 10X minimum inhibition concentration (MIC), using our previous procedure.[30] Intracellular bacteria were produced by exposing J774 macrophages to MRSA USA400 cells at a multiplicity of infection of 1:10 for 1 h, followed by treatment with gentamicin (200 μg/mL) to kill extracellular MRSA as described elsewhere.[31] Intracellular bacteria were recovered post-aPDT by the lysis of washed J774 cells with 0.1% TX-100, followed quickly by serial dilution and plating.

Cytotoxicity studies. HaCaT and J774 cells were obtained from AddexBio and cultured in Dulbecco's Modified Eagle Medium (DMEM) supplemented with 10% FBS at 37 °C in a 5% CO_2 atmosphere. Cells were incubated in 96-well microtiter plates (10^4 cells/well) and treated with 10-nm GaHb–AgNPs, with final concentrations ranging from 5.8 to 46 μg/mL, followed by 405-nm irradiation and 24-h incubation at 37 °C. Cell viabilities were quantified using the MTT assay; detailed procedures are described in the ESI.

Results and discussion

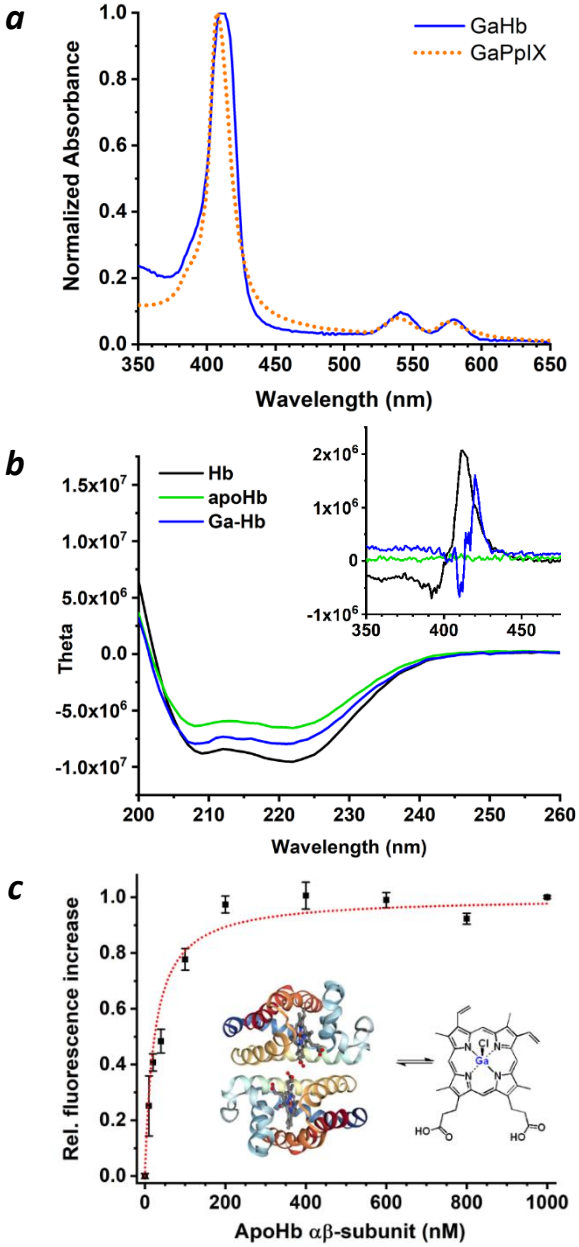

Figure 2. Characterization of GaHb. (a) Absorbance spectra of GaPpIX and GaHb; (b) circular dichroism spectra of Hb, apoHb, and GaHb at UV and visible wavelengths (*inset*); (c) FP assay of GaPpIX binding by apoHb (αβ dimer form[32]) with K_a = 0.042 nM^{-1} (K_d = 48 nM per subunit).

Characterization of GaHb and GaHb–AgNPs. Native Hb exists as an $\alpha_2\beta_2$ tetramer with a haeme-binding pocket for each subunit, and dissociates reversibly into αβ dimers in dilute solution.[33,34] Characterization of reconstituted GaHb by gel electrophoresis, UV-vis spectroscopy, and CD indicated their reassembly into αβ dimers and tetramers with retention of global structure, and a 10-nm shift in the Soret band relative to free GaPpIX (λ_{max} 416 nm; **Figure 2** and ESI). The dissociation constant (K_d) of GaPpIX and apoHb was measured to be 48 nM by fluorescence polarization, which is higher than that of hemin ($K_d \leq 42$ pM)[24] but sufficient to form a stable complex.

GaHb and citrate-stabilized 10-nm AgNPs (d_h ~14 nm by DLS) were incubated in PBS (pH 7.4) at 4 °C, then centrifuged gently to remove excess GaHb and redispersed in borate buffer (pH 8.5). A Bradford assay indicated a Ag:Hb weight ratio of 7.4, corresponding to a mean of 7 GaHb (and 28 GaPpIX) per 10-nm AgNP (see ESI). DLS and absorption spectroscopy respectively indicated a 20% increase in hydrodynamic size (d_h) to 17 nm, and a 3-nm redshift in λ_{max} to 396 nm (FWHM = 59 nm). This is in accord with negative-stain TEM images of GaHb–AgNPs, which reveal coronae suggestive of GaHb monolayers (**Figure 3**). GaHb–AgNP constructs were also prepared using 40-nm AgNPs (d_h ~36 nm), with similarly modest changes in d_h and λ_{max} and a Ag:Hb weight ratio of 4.8 (688 GaHb per 40-nm AgNP; see ESI).

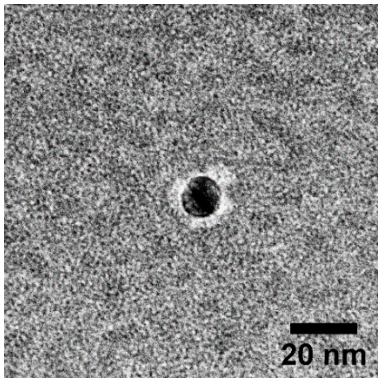

Figure 3. Negative-stain TEM image of GaHb-AgNP (Tecnai T20, 200 kV), using 1% phosphotungstic acid on a carbon-coated Formvar grid.

Photodynamic activity of GaHb–AgNPs. To establish their potential for aPDT, GaHb–AgNPs were characterized for their capacity to generate $^1O_2$ at 405 nm, which overlaps with the plasmon resonance of AgNPs. The efficiency of $^1O_2$ production was quantified by ESR via the generation of nitroxyl radicals[35] and normalized against the activity of GaPpIX, whose $^1O_2$ quantum yield was determined recently (Φ_Δ = 0.45).[14] ESR measurements were obtained for GaHb alone, GaHb–AgNPs using 10- and 40-nm AgNPs, and also for citrate-stabilized 10-nm AgNPs, which did not yield any positive ESR signals after 405-nm irradiation despite earlier reports[36] (**Figure 4** and **Table 1**). Nitroxyl generation by GaHb (per unit of GaPpIX) was not as efficient as the free PS, presumably due to interference by Hb itself. In contrast, large enhancements in ESR signals were observed with GaHb–AgNPs, particularly with 10-nm cores. The nearly 5-fold enhancement provided by AgNPs can be

considered as a lower estimate, given the partial interference by Hb.

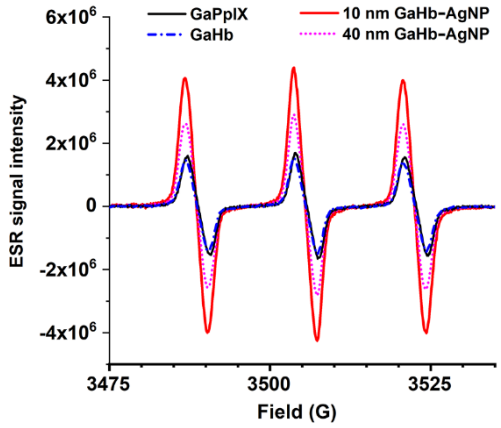

Figure 4. ESR spectra of nitroxyl radicals generated by GaPpIX, GaHb, and GaHb–AgNP (10 and 40 nm).

Table 1. Efficiency of $^1O_2$ generation by GaHb–AgNPs, relative to GaPpIX

Photosensitizer	Relative efficiency[a]
GaPpIX	1.00
GaHb	0.77
GaHb–AgNP (10 nm)	4.59
GaHb–AgNP (40 nm)	2.64
AgNP (10 nm)	--

[a] Based on integration of ESR nitroxyl signals, generated in the presence of photosensitizers after 10-s irradiation by a 405-nm LED source (140 mW/cm^2). Values were scaled and normalized according to amount of GaPpIX in each sample.

GaHb–AgNPs were then evaluated as aPDT agents against a strain of *S. aureus* (PC 1203), exposed for 10 seconds to the 405-nm LED source (fluence = 1.4 J/cm^2). As anticipated, GaHb–AgNPs with 10-nm cores were highly active, with MBC (99.9% reduction in CFU count) between 2.9 and 4.1 μg/mL (**Figure 5a**). When converted into GaPpIX equivalents (28 units per AgNP), this activity translates into values between 21 and 29 nM, slightly lower than the MBC for GaPpIX alone (>30 nM).[14] More remarkably, GaHb–AgNP mediated the complete eradication (>6-log reduction) of *S. aureus* at a slightly higher loading of 5.8 μg/mL, or 41 nM in GaPpIX units. A comparison between GaHb–AgNP, GaHb, and free GaPpIX at equivalent PS loadings (27.5 ng/mL GaPpIX) revealed differences in potency of over 3 orders of magnitude for bacterial eradication (**Figure 5b**). Exposure to AgNPs and 405-nm light produced only modest decreases in bacterial count (0.3-log reduction). Lastly, the dark toxicity of GaHb–AgNPs was negligible at the loadings used in this study, confirming that the antimicrobial potency of GaHb–AgNP is essentially due to photodynamic inactivation. We note that GaHb–AgNPs with 40-nm cores were much less active than those with 10-nm cores, which will be discussed later.

GaHb–AgNPs were also tested against several clinical isolates of MRSA strains (**Figure 5a**). These were comparable to the *S. aureus* PC 1203 strain in their susceptibility to GaPpIX-mediated aPDT,[14] but exhibited greater variance to photodynamic inactivation by GaHb–AgNP. Nevertheless, eradication could be achieved with a 10-second light exposure using as little as 16.3 μg/mL GaHb–AgNP.

To determine whether GaHb–AgNPs could be used against non-growing dormant persister cells whose responses to conventional antibiotics are inert, MRSA USA300 (NRS 384) was first treated with ciprofloxacin at 10X MIC, followed by cultivation of surviving cells.[30] These were then treated with 4.1 μg/mL GaHb–AgNP and exposed to the 405-nm LED source for 10 seconds, which resulted in a 2.7-log reduction in CFU count (**Figure 5a**). In comparison, persisters treated with GaHb–AgNPs without light exposure (dark toxicity control) experienced only a 0.3-log reduction. This validates the efficacy of GaHb–AgNPs for aPDT against bacterial persisters with acquired drug resistance.

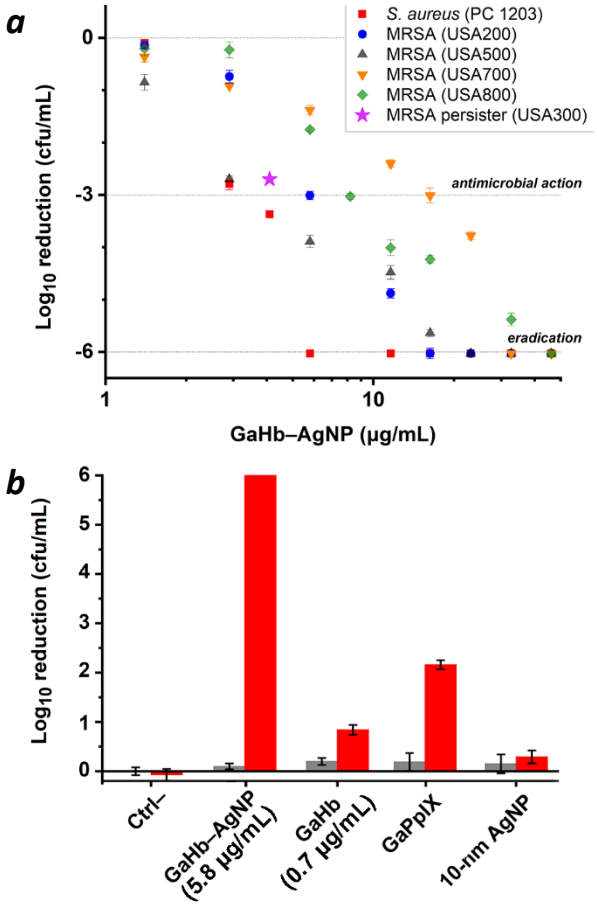

Figure 5. (a) Photodynamic inactivation of *S. aureus* (PC 1203) and several MRSA strains (NRS 383–387) using 10-nm GaHb–AgNPs, following 10-s exposure to 405-nm light (1.4 J/cm^2). Eradication (>6-log reduction) of PC 1203 was observed at 5.8 μg/mL (*N*=3). (b) Comparison of GaHb–AgNP against its components at a constant level of GaPpIX (27.5 ng/mL), for aPDI of *S. aureus* (PC 1203). Dark toxicities (grey bars) included for comparison.

GaHb–AgNPs were also evaluated for aPDT activity against intracellular bacteria residing within macrophages, which play a central role in the immune response against bacterial infection.[37] Paradoxically, engulfed bacteria are often capable of evading phagocytosis and can proliferate within host macrophages.[38] To determine whether aPDT might have an

effect against internalized bacteria, J774 cells infected with MRSA USA 400 were treated with GaHb–AgNPs (46 µg/mL), followed 5 minutes or 24 hours later with a 10-second exposure to 405-nm light (**Figure 6**). The population of intracellular MRSA experienced a 1.3-log reduction (95%) with immediate irradiation, but a 0.8-log reduction if irradiation was delayed by one day and a 0.6-log reduction without light (dark toxicity). The aPDT effect was mostly lost at lower GaHb–AgNP concentrations, which appeared to stimulate only modest levels of phagocytic activity. It is unclear to what extent GaHb–AgNPs are delivered to intracellular MRSA, however it is well documented that metal nanoparticles can enhance innate immune response by inducing macrophage polarization.[39,40] Photocatalytic ROS generation may thus be contributing toward responses that disrupt intracellular homeostasis within host macrophages, perhaps via upregulation of lysosomal activity.

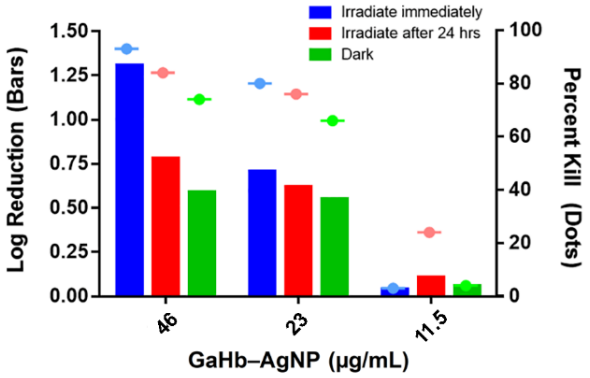

Figure 6. Photodynamic inactivation of intracellular MRSA using GaHb–AgNP and the 405-nm LED source (1.4 J/cm^2), applied immediately or 24 hours after treatment. Results presented in units of log reduction (solid bars) or percent kill (dashed dots).

To determine whether 10-nm GaHb–AgNPs might cause cytotoxicity during aPDT applied toward skin wound infections, cell viability assays were performed using keratinocytes (HaCaT) (**Figure 7a** and ESI) and J774 macrophages (**Figure 7b**). Dark toxicity was evaluated by MTT assay, with no adverse effects observed for HaCaT cells at the highest concentrations used (46 µg/mL). In fact, GaHb–AgNPs promoted cell activity, possibly stimulated by low levels of ROS production at non-lethal levels. Previous studies have shown that ROS can be positive regulators of cellular function, homeostasis and growth factor responses.[41]

The photodynamic effect of 10-nm GaHb–AgNPs on HaCaT cell viability was evaluated following a 10-second exposure to the 405-nm LED source using 23 or 46 µg/mL GaHb–AgNP, corresponding with the concentrations used for intracellular aPDT (**Figure 6**). The 405-nm irradiation caused a marked increase in mitochondrial activity in the control and 23 µg/mL experiments (**Figure 7a**); adding a 24-hour delay between GaHb–AgNP addition and irradiation further amplified this effect (see ESI). Keratinocyte activity is well known to be stimulated by light, a likely basis for low-level light therapies.[42]

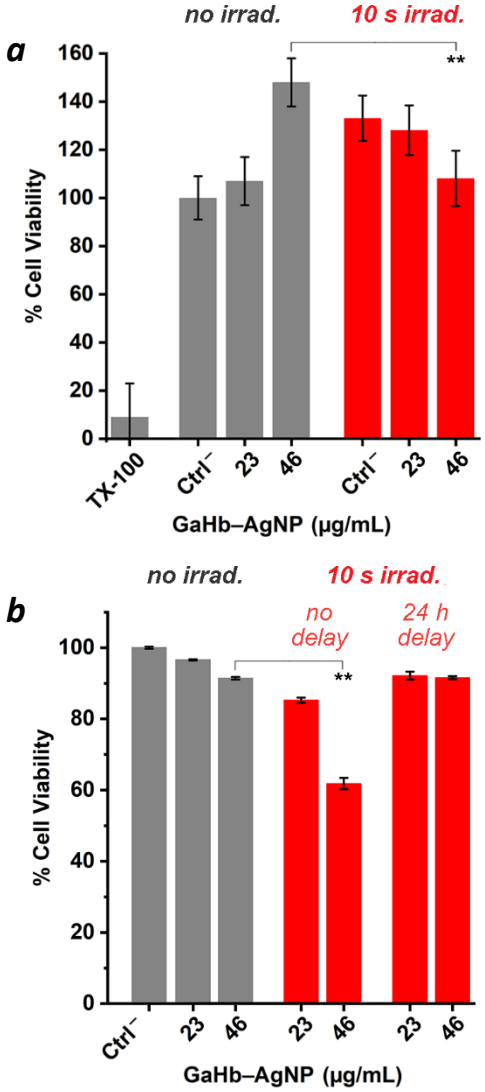

Figure 7. (a) Cell viability (MTT) assays using 10-nm GaHb-AgNPs against HaCaT cells, without and with exposure to 405-nm LED source (10 s, 1.4 J/cm^2; N = 3). Controls include cells treated with 0.005% Triton X-100, and cells without GaHb-AgNPs (Ctrl$^-$). (b) MTT assay using J774 macrophages, with 0- or 24-h delay between GaHb–AgNP treatment and light exposure. ** $p < 0.05$.

In the context of cell phototoxicity, no adverse effect was observed with 23 µg/mL GaHb–AgNPs, but a 25% loss in activity occurred with 46 µg/mL (**Figure 7a**, $p < 0.05$). The dichotomous effect of GaHb–AgNPs with and without light supports the notion that cells are sensitive to ROS concentrations, with a fine line drawn between oxidative damage and stress-induced growth.[41] Overall, these tests indicate that GaHb–AgNPs have low toxicity toward skin cells under aPDT conditions, and support their exploration as therapeutic agents for future *in vivo* studies.

GaHb–AgNPs showed only modest dark toxicity toward J774 macrophages, but caused greater loss in mitochondrial activity following a 10-s exposure to 405-nm irradiation ($p < 0.05$; **Figure 7b**). Phototoxicity could be neutralized by delaying light irradiation by 24 hours, albeit at the expense of antimicrobial activity (**Figure 6**). We thus anticipate that dermal tissues treated should be compatible with aPDT when using GaHb–

AgNPs at relatively high doses, but may experience a temporary reduction in local macrophage count. The effects of GaHb–AgNPs on neutrophils and other cells in the innate immune response remain to be investigated.

To determine whether GaHb–AgNPs could mediate aPDT at lower irradiation intensities, studies were performed using a 20-W CFL with a major emission line at 406 nm. 3- and 6-log reductions of *S. aureus* could be achieved within 15 min using 16.3 and 32.7 μg/mL GaHb–AgNP, respectively (**Figure 8**). Comparable results were obtained against clinical MRSA strains with a 15-min exposure, at GaHb–AgNP concentrations as low as 11.6 μg/mL for antimicrobial activity and 16.3 μg/mL for eradication. This supports the possibility of administering aPDT with GaHb–AgNPs using inexpensive light sources.

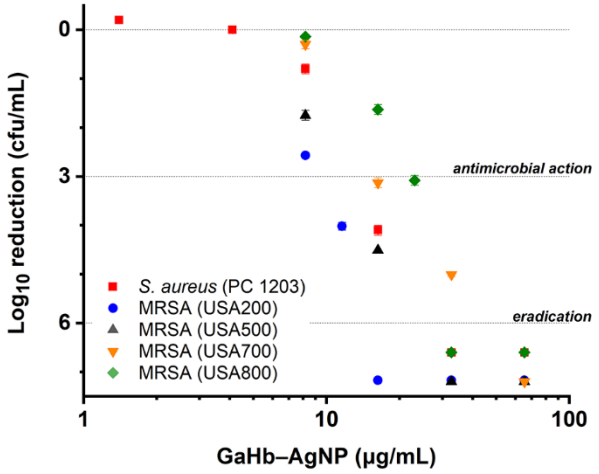

Figure 8. Photodynamic inactivation of *S. aureus* (PC 1203) and MRSA strains using 10-nm GaHb–AgNPs, following 15-min exposure to a 20-W CFL (λ_{max} = 406 nm).

Mechanistic insights of GaHb–AgNP activity. The studies above strongly suggest that the aPDT potency of GaHb is enhanced by plasmon-resonant coupling with 10-nm AgNPs. Experiments with GaHb adsorbed onto 10-nm AuNPs (characterization in ESI) show greatly reduced activity, with only 1-log reduction using the CFL source at 70 μg/mL GaHb–AuNP, the highest concentration used (**Figure 9a**). The plasmon band of AuNPs is lower than that of AgNPs, and may quench $^1O_2$ and ROS production by energy transfer from excited-state GaPpIX.

The size of the GaHb–AgNP is also important, an observation that has been made in other bactericidal studies using AgNPs.[43] Increasing the AgNP core to 40 nm reduced aPDI activity to modest levels even at 115 μg/mL, the highest concentration used (**Figure 9a**). This leads us to postulate that the interaction between GaHb–AgNPs and cell-surface hemin receptors on the bacteria wall is size-dependent. It should be noted that despite evidence for plasmon-enhanced $^1O_2$ generation by 40-nm GaHb–AgNPs (**Table 1**), a strong plasmon band can also promote other physical processes that are detrimental to photosensitization, such as resonant energy transfer or radiative pathways for photoemission, at the expense of intersystem crossing.[44]

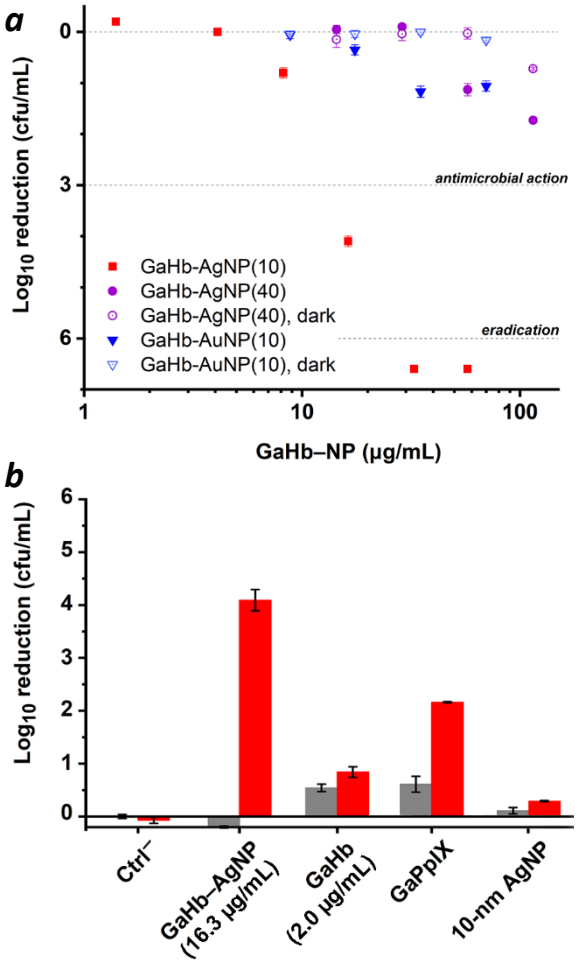

Figure 9. (a) Photodynamic activities of 10-nm GaHb–AuNPs (blue) and 40-nm GaHb–AgNPs (purple) on a per weight basis against *S. aureus*, following 15-min exposure to a 20-W CFL (λ_{max} = 406 nm). Activities for 10-nm GaHb–AgNPs (red) and GaHb–NPs without light (open symbols) included for comparison. (b) Photodynamic activities of various species (red bars) at equal loadings of GaPpIX (78 ng/mL). Dark toxicities (grey bars) included for comparison.

To further confirm the superior aPDT potency of 10-nm GaHb–AgNPs against *S. aureus*, a direct comparison was made with GaHb and GaPpIX at equivalent PS loadings using the 20-W CFL source (**Figure 9b**). 10-nm GaHb–AgNPs (16.3 μg/mL) produced a 4.1-log reduction of *S. aureus* with a 15-minute exposure to the 20-W CFL, whereas GaPpIX (78 ng/mL) and GaHb (2.0 μg/mL) produced only a 1.3- and 0.8-log reduction respectively, and also exhibited higher dark toxicities. Again, this establishes that 10-nm GaHb–AgNPs are uniquely potent aPDT agents.

With respect to the speed of aPDT action, prior studies with GaPpIX lead us to presume that GaHb–AgNP delivery to *S. aureus* is diffusion-limited,[14] with oxidative damage of the cell wall being the main cause of cell death. Chemical SEM imaging using EDS revealed a uniform GaHb–AgNP distribution on the cell walls of *S. aureus* following a 30-min exposure (**Figure 10a,b**). To determine whether GaHb–AgNPs could be internalized at all by *S. aureus*, bacteria were incubated with GaHb–AgNPs for 1 hour in the dark, then washed, fixed, and sectioned by microtomy for TEM image analysis (**Figure 10c**). In

nearly all sections examined, GaHb–AgNPs could only be found on the outer wall of *S. aureus*, and are thus unlikely to be internalized prior to aPDT. This again supports our notion that the bacterial cell wall is the primary target of photo-oxidation. In this regard, some earlier studies indicate that AgNPs smaller than 10 nm are able to permeate MRSA[45] as well as Gram-negative bacteria like *E. coli*,[43,46] with local damage to the outer membrane.

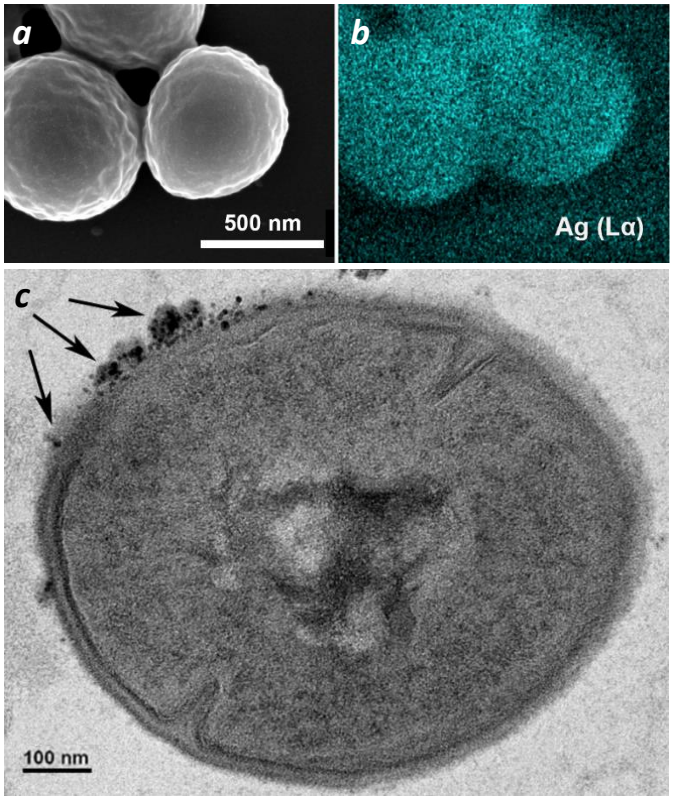

Figure 10. (a,b) SEM and EDS (Ag Lα) images of *S. aureus* after a 30-min exposure to 10-nm GaHb–AgNPs. (c) TEM image of GaHb–AgNPs (indicated with arrows) on the outer bacterial wall (additional images in ESI). TEM sample was prepared using *S. aureus* exposed to GaHb–AgNPs for 1 hour, then sectioned by microtomy.

Finally, it is interesting to compare the aPDT activity of GaHb–AgNPs in the context of earlier antimicrobial studies involving NP-based agents, most of which are also known for ROS generation (**Table 2**). For practical reasons, our selection is restricted to inorganic NPs whose bactericidal effects or MBC values have been quantified by reduction in colony counts of plated serial dilutions.[47] Such comparisons are intended to be qualitative rather than quantitative, as bacterial strains, NP types, and NP concentrations vary widely between studies.[48] Nevertheless, we note that GaHb–AgNPs rank among the most potent antimicrobial NPs when compared on a per weight basis, including other UV-active photosensitizers[49,50,51] or PS carriers.[17] We attribute the superior potency of GaHb–AgNPs to their recognition by Isd receptors expressed by *S. aureus*, which have high affinity for Hb and other haemoproteins as well as hemin itself.[26]

Table 2. Antimicrobial activities of inorganic NPs (select examples)

NP type	bacteria species	Log reduction[a]	Concentration (μg/mL)
ZnO (12, 45 nm)[52]	*E. coli*	2	4,100 [b]
colloidal ZnO + UV[49]	*E. coli*	6	2,000
ZnO (8 nm) + light[51]	*S. aureus*/MRSA	2	163 [b]
ZnO pyramids (<20 nm)[53]	*S. aureus*/MRSA	4	400
ZnO (<50 nm)[54]	*C. jejuni*	3	25
$Zn_{0.9}$ $Fe_{0.1}O$ (11 nm)[55]	*S. aureus*	6	300
colloidal TiO_2 + UV[49]	*E. coli*	6	2,000
CuO (48 nm)[54]	*C. jejuni*	3	6.3
Cu (9.3 nm)[56]	*E. coli*	3	160
Ag_2O (17.5 nm)[57]	*E. coli* *P. aeruginosa*	3	18
Ag (3.3 nm)[56]	*E. coli*	3	60
Ag (3.3 nm) [56]	*S. aureus*	3	160
Ag (21 nm)[54]	*Salmonella ssp.*	3	50
Ag (21 nm)[54]	*C. jejuni*	3	6.3
Ag@SiO_2–HPIX + light[17]	*E. coli* *A. baumannii*	6	24.5 [b]
This work	***S. aureus*/MRSA**	**6**	**5.8**

[a] Based on CFU/mL of plated serial dilutions. [b] Value derived from quantities provided in studies.

Conclusions

The antimicrobial photodynamic activity of GaPpIX is amplified manifold when coupled with 10-nm AgNPs, using haemoglobin as a host protein. Reconstituted GaHb is structurally stable and adsorbs onto 10-nm AgNPs in a 7:1 ratio on average, corresponding to 28 GaPpIX units per particle. GaHb–AgNPs are potent aPDT agents against *S. aureus* and MRSA, with MBC values (3-log reduction) of 4–16 μg/mL following a 10-second exposure to 405-nm light (1.4 J/cm^2). Eradication (>6-log reduction) can be achieved at GaHb–AgNP levels as low as 5.8 μg/mL, which compares favourably against the most active antimicrobial NPs studied to date. GaHb–AgNPs are also active against persister MRSA and intracellular MRSA, and remain highly potent even when using inexpensive light sources, while exhibiting low cytotoxicity against keratinocytes. The antimicrobial activity of GaHb–AgNPs is size-dependent and appears to be directed against the bacterial outer wall, supporting our belief that local photo-oxidation is mediated by their binding to haemoprotein receptors on the bacteria surface.

Conflicts of interest

There are no conflicts to declare.

Acknowledgements

We gratefully acknowledge support from the National Science Foundation (CMMI-1449358), the National Institutes of Health (R01 AI130186), and the Purdue University Center for Cancer Research (P30 CA023168). We thank BEI Resources at NIAID for

providing several of the bacterial strains used in this study, Pat Bishop for assistance with CD, Hartmut Hedderich for advice on photophysical studies, Robert Seiler and Chris Gilpin for microtomy and TEM imaging, and Lan Chen in the Chemical Genomics Facility for assistance with FP assays.

Notes and references

[1] A. P. Kourtis, K. Hatfield, J. Baggs, Y. Mu, I. See, E. Epson, J. Nadle, M. A. Kainer, G. Dumyati, S. Petit, et al., *MMWR Morb. Mortal. Wkly. Rep.*, 2019, **68**, 214.
[2] S. S. Magill, E. O'Leary, S. J. Janelle, D. L. Thompson, G. Dumyati, J. Nadle, L. E. Wilson, M. A. Kainer, R. Lynfield, S. Greissman, et al., *New Engl. J. Med.*, 2018, **379**, 1732.
[3] K. W. McConeghy, D. J. Mikolich, K. L. LaPlante, *Pharmacotherapy* **29**, 263-280 (2009).
[4] M. K. Hayden, K. Lolans, K. Haffenreffer, T. R. Avery, K. Kleinman, H. Li, R. E. Kaganov, J. Lankiewicz, J. Moody, E. Septimus, et al., *J. Clin. Microbiol.*, 2016, **54**, 2735.
[5] M. R. Hamblin and T. Hasan, *Photochem. Photobiol. Sci.*, 2004, **3**, 436.
[6] F. Cieplik, D. Deng, W. Crielaard, W. Buchalla, E. Hellwig, A. Al-Ahmad and T. Maisch, *Crit. Rev. Microbiol.*, 2018, **44**, 571.
[7] J. A. Imlay, *Nat. Rev. Microbiol.*, 2013, **11**, 443.
[8] F. Wilkinson, W. P. Helman and A. B. Ross, *J. Phys. Chem. Ref. Data*, 1995, **24**, 663.
[9] T. Maisch, *Photochem. Photobiol. Sci.*, 2015, **14**, 1518.
[10] M. Wainwright, T. Maisch, S. Nonell, K. Plaetzer, A. Almeida, G. P. Tegos and M. R. Hamblin, *Lancet Infect. Dis.*, 2017, **17**, e49.
[11] A. Rapacka-Zdonczyk, A. Wozniak, M. Pieranski, A. Woziwodzka, K. P. Bielawski and M. Grinholc, *Sci. Rep.*, 2019, **9**, 9423.
[12] M. Wainwright, *J. Antimicrob. Chemother.*, 1998, **42**, 13.
[13] T. R. Maltais, A. Adak, W. Younis, M. N. Seleem and A. Wei, *Bioconjugate Chem.*, 2016, **27**, 1713.
[14] A. V. Morales-de-Echegaray, T. R. Maltais, L. Lin, W. Younis, N. R. Kadasala, M. N. Seleem and A. Wei, *ACS Infect. Dis.*, 2018, **4**, 1564.
[15] Y. Zhang, K. Aslan, M. J. R. Previte and C. D. Geddes, *Proc. Natl. Acad. Sci. U.S.A.*, 2008, **105**, 1798.
[16] O. Planas, N. Macia, M. Agut, S. Nonell and B. Heyne, *J. Am. Chem. Soc.*, 2016, **138**, 2762.
[17] B. Hu, X. Cao, K. Nahan, J. Caruso, H. Tang and P. Zhang, *J. Mater. Chem. B*, 2014, **2**, 7073.
[18] M. Lismont, L. Dreesen, B. Heinrichs and C. A. Páez, *Photochem. Photobiol.*, 2016, **92**, 247.
[19] C. Wang, Q. Cui, X. Wang and L. Li, *ACS Appl. Mater. Interfaces*, 2016, **8**, 29101.
[20] P. García Calavia, M. J. Marín, I. Chambrier, M. J. Cook and D. A. Russell, *Photochem. Photobiol. Sci.*, 2018, **17**, 281.
[21] N. Nombona, E. Antunes, W. Chidawanyika, P. Kleyi, Z. Tshentu and T. Nyokong, *J. Photochem. Photobiol. A*, 2012, **233**, 24.
[22] R. Ding, X. Yu, P. Wang, J. Zhang, Y. Zhou, X. Cao, H. Tang, N. Ayres and P. Zhang, *RSC Adv.*, 2016, **6**, 20392.
[23] A. Wei, J. G. Mehtala and A. K. Patri, *J. Control. Release*, 2012, **164**, 236.
[24] M. S. Hargrove, T. Whitaker, J. S. Olson, R. J. Vali and A. J. Mathews, *J. Biol. Chem.*, 1997, **272**, 17385.
[25] S. Tenzer, D. Docter, J. Kuharev, A. Musyanovych, V. Fetz, R. Hecht, F. Schlenk, D. Fischer, K. Kiouptsi, C. Reinhardt, et al., *Nat. Nanotechnol.*, 2013, **8**, 772.
[26] N. D. Hammer and E. P. Skaar, *Annu. Rev. Microbiol.*, 2011, **65**, 129.
[27] S. Zhang, S. Ding, J. Yu, X. Chen, Q. Lei and W. Fang, *Langmuir*, 2015, **31**, 12161.
[28] F. Ascoli, M. R. Rossi Fanelli and E. Antonini, in *Methods in Enzymology*, Academic Press, 1981, Vol. 76, Ch. 5, 72.
[29] S. Xu and I. A. Kaltashov, *J. Am. Soc. Mass Spectrom.*, 2016, **27**, 2025.
[30] (a) S. Thangamani, H. Mohammad, M. F. N. Abushahba, T. J. P. Sobreira and M. N. Seleem, *Int. J. Antimicrob. Agents*, 2016, **47**, 195. (b) M. F. Mohamed, A. Abdelkhalek and M. N. Seleem, *Sci. Rep.*, 2016, **6**, 29707.
[31] (a) A. Hammad, N.S. Abutaleb, M.M. Elsebaei, A.B. Norvil, M. Alswah, A.O. Ali, J.A. Abdel-Aleem, A. Alattar, S.A. Bayoumi, H. Gowher, et al., *J. Med. Chem.* 2019, **62**, 7998. (b) M.M. Elsebaei, N.S. Abutaleb, A.A. Mahgoub, D. Li, M. Hagras, H. Mohammad, M.N. Seleem and A.S. Mayhoub, *Eur. J. Med. Chem.,* 2019, **182**, 111593.
[32] W. E. Royer, *J. Mol. Biol.*, 1994, **235**, 657 (PDB:3SDH).
[33] S. L. White, *J. Biol. Chem.*, 1975, **250**, 1263.
[34] P. Hensley, S. J. Edelstein, D. C. Wharton and Q. H. Gibson, *J. Biol. Chem.*, 1975, **250**, 952.
[35] K. Nakamura, K. Ishiyama, H. Ikai, T. Kanno, K. Sasaki, Y. Niwano and M. Kohno, *J. Clin. Biochem. Nutr.*, 2011, **49**, 87.
[36] It has been shown that $^1O_2$ can be generated from metal NPs without organic PS, using an irradiation time of 8 h. See:

R. Vankayala, A. Sagadevan, P. Vijayaraghavan, C.-L. Kuo and K. C. Hwang, *Angew. Chem. Int. Ed.*, 2011, **50**, 10640.
[37] G. Weiss and U. E. Schaible, *Immunol. Rev.*, 2015, **264**, 182.
[38] G. Mitchell, C. Chen and D. A. Portnoy, *Microbiol Spectr.*, 2016, **4**, MCHD-0012-2015.
[39] Y. Liu, J. Hardie, X. Zhang and V. M. Rotello, *Sem. Immunol.*, 2017, **34**, 25.
[40] D. Boraschi, P. Italiani, R. Palomba, P. Decuzzi, A. Duschl, B. Fadeel and S. M. Moghimi, *Sem. Immunol.*, 2017, **34**, 33.
[41] M. Schieber and N. S. Chandel, *Curr. Biol.*, 2014, **24**, R453.
[42] J. Hashmi, Y. Huang, S. Sharma, D. Kurup, L. De Taboada, J. Carroll and M. Hamblin, *Lasers Surg. Med.*, 2010, **42**, 450.
[43] J. R. Morones, J. L. Elechiguerra, A. Camacho, K. Holt, J. B. Kouri, J. T. Ramírez and M. J. Yacaman, *Nanotechnology*, 2005, **16**, 2346.
[44] M. Bauch, K. Toma, M. Toma, Q. Zhang and J. Dostalek, *Plasmonics*, 2014, **9**, 781.
[45] D. G. Romero-Urbina, H. H. Lara, J. J. Velázquez-Salazar, M. J. Arellano-Jiménez, E. Larios, A. Srinivasan, J. L. Lopez-Ribot and M. J. Yacamán, *Beilstein J. Nanotechnol.*, 2015, **6**, 2396.
[46] I. Sondi and B. Salopek-Sondi, *J. Colloid Interface Sci.*, 2004, **275**, 177.
[47] A. L. Barry, W. A. Craig, H. Nadler, L. B. Reller, C. C. Sanders and J. M. Swenson, Methods for determining bactericidal activity of antimicrobial agents: Approved guideline. *NCCLS document M26-A*, 1999, **19**, 1.
[48] U. Kadiyala, N. A. Kotov and J. S. VanEpps, *Curr. Pharm. Des.*, 2018, **24**, 896.
[49] H.-L. Liu and T. C. K. Yang, *Process Biochem.*, 2003, **39**, 475.
[50] H. A. Foster, I. B. Ditta, S. Varghese and A. Steele, *Appl. Microbiol. Biotechnol.*, 2011, **90**, 1847.
[51] N. Jones, B. Ray, K. T. Ranjit and A. C. Manna, *FEMS Microbiol. Lett.*, 2008, **279**, 71.
[52] N. Padmavathy and R. Vijayaraghavan, *Sci. Technol. Adv. Mater.*, 2008, **9**, 035004.
[53] U. Kadiyala, E. S. Turali-Emre, J. H. Bahng, N. A. Kotov and J. S. VanEpps, *Nanoscale*, 2018, **10**, 4927.
[54] L. L. Duffy, M. J. Osmond-McLeod, J. Judy and T. King, *Food Control*, 2018, **92**, 293.
[55] T. Gordon, B. Perlstein, O. Houbara, I. Felner, E. Banin and S. Margel, *Colloid. Surf. A*, 2011, **374**, 1.
[56] J. P. Ruparelia, A. K. Chatterjee, S. P. Duttagupta and S. Mukherji, *Acta Biomater.*, 2008, **4**, 707.
[57] H. Negi, P. Rathinavelu Saravanan, T. Agarwal, M. Ghulam Haider Zaidi and R. Goel, *J. Gen. Appl. Microbiol.*, 2013, **59**, 83.